Increasing electrostatic stabilization of the nitride anion in high-pressure modifications of Li_3N and Na_3N due to coordination changes might indicate a route to stabilize even more labile nitrides of K, Rb, and Cs by preparing them under high-pressure conditions.

[1] *Fischer, D. and M. Jansen.* Angewandte Chemie **114**, 1831–1833 (2002).

[2] *Vajenine, G.V.* Inorganic Chemistry **46**, 5146–5148 (2007).

[3] *Rabenau, A. and H. Schulz.* Journal of the Less-Common Metals **50**, 155–159 (1976).

[4] *Beister, H.J., S. Haag, R. Kniep, K. Strössner and K. Syassen.* Angewandte Chemie **100**, 1116–1118 (1988).

[5] *Lazicki, A., B. Maddox, W.J. Evans, C.-S. Yoo, A.K. McMahan, W.E. Pickett, R.T. Scalettar, M.Y. Hu and P. Chow.* Physical Review Letters **95**, 165503 (2005).

[6] *Schön, J.C., M.A.C. Wevers and M. Jansen.* Journal of Materials Chemistry **11**, 69–77 (2001).

The high-pressure crystal structure of the NLO compound BiB_3O_6 from 2D powder diffraction data

R.E. Dinnebier, B. Hinrichsen and M. Jansen; A. Lennie (Daresbury Laboratory, United Kingdom)

As part of a long term project on the effect of stereochemically active lone pairs on crystal structures at high pressure, α-bismuth borate was studied in the pressure range from ambient pressure to 11.6 GPa. In general, lone pairs can be viewed as pseudo-ligands in compounds exhibiting increasingly covalent bonding contributions, significantly changing the space requirements and bonding situation in the affected solids. As these crystal structures are rather open, it can be expected that such compounds undergo pressure induced phase transitions. In general, high-pressure powder diffraction data from DAC's (diamond anvil cell) are often difficult to interpret due to the fact that usually very few extremely intense spikes, originating from grains in an ideal diffraction position tend to dominate the diffraction pattern. Therefore, we developed a phenomenological model for the description of such intensity distributions which we applied here to extract normally distributed intensities using well-known fractile filters.

The crystal structure of the lone pair bearing compound α-BiB_3O_6 has recently attracted considerable interest as a polar, non-ferroelectric compound with exceptional non-linear optical (NLO) properties. A technical application is possible, since single crystals of sufficient size and quality could be synthesized. The crystal structure of α-BiB_3O_6 at ambient conditions can be described as a phylloborate layer structure consisting of alternating layers of borate anions and bismuth cations perpendicular to *c*-axis. The borate groups consisting of BO_3 triangles and BO_4 tetrahedra in a 2:1 ratio form a 2-dimensional net linked by corners. The coordination of the BiO_6 polyhedron is highly irregular, due to the non-bonding lone pair electrons of the sp^3 hybridized Bi^{3+} orbitals. The NLO properties were attributed to the bonds in the triangular [BO_3] units and to the lone pair at the Bi^{+3} cation. α-BiB_3O_6 exhibits one of the largest anisotropies in the elastic constants and the thermal expansion observed in ionic crystals, anisotropy which is attributed to the preferential orientation of the lone electron pair of Bi^{3+}. In the temperature range from 8 K to 999 K, no structural phase transition was found for α-BiB_3O_6. Preliminary investigations using Raman spectroscopy at room temperature and elevated pressure did not show any evidence for structural changes up to a pressure of $p = 18$ GPa.

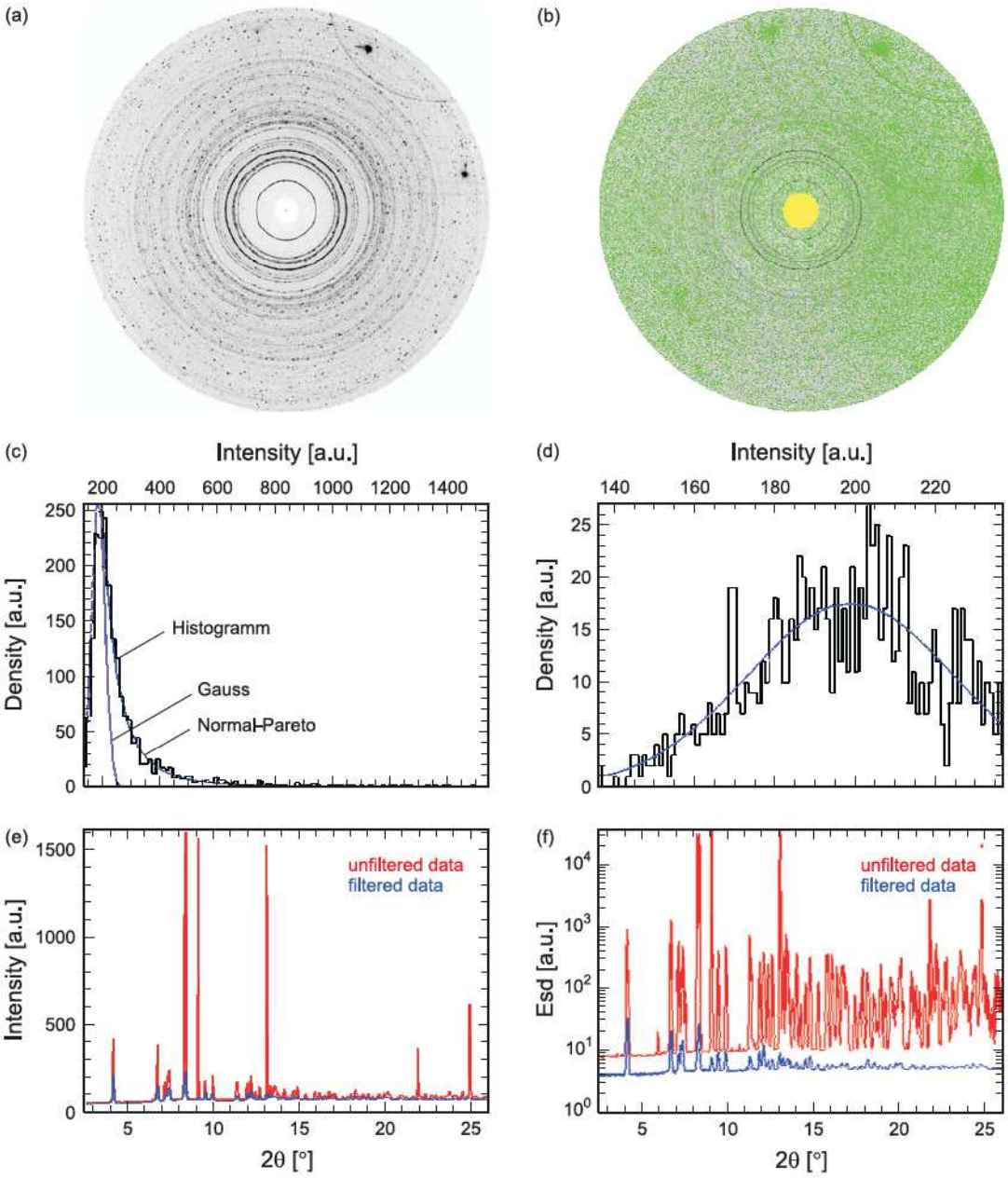

Figure 41: Powder diffraction data of ε-BiB_3O_4 at $P = 8.35$ GPa, collected by a two-dimensional image plate detector. The raw image (a) and the filtered image (b) are shown. The green mask represents the pixels which belong to the top 48% of the intensities per integration bin. The blue mask shows the pixels which belong to the bottom 2% of the intensities per integration bin. The yellow mask is the beam stop mask filtering the first 2° 2θ of the diffraction image. Only the uncolored region of the image is used for the integration to a 1D diffractogram. The intensity distribution of an unfiltered (c) and filtered (d) bin is displayed showing fits to the expected normal and the proposed normal-Pareto distribution. The effect of filtering is further visualized on the final integrated and background corrected pattern (e) and on the standard deviations (f) (In red the integrated pattern of the unfiltered image, in blue the diffractogram of the filtered image).

Because of the high compressibility due to the lone pair of the Bi^{3+} cation and the extreme anisotropy of the thermal expansion, we decided to investigate the pressure dependence of the crystal structure of α-BiB_3O_6, a study which we consider a prerequisite for future investigations of additional possibly quenchable high-pressure modifications. For this purpose, *in situ* high-pressure powder diffraction experiments using a diamond anvil cell (DAC) were performed at the high-flux powder diffraction Station 9.5HPT of Daresbury Laboratory, U.K, equipped with a MAR345 image plate detector. The image plate orientation and sample to plate distance were determined using a silicon powder standard (NIST 640b). Initially, a traditional calibration routine was run using the Powder3D IP software. The results were later refined using the whole image refinement (WIR) procedure. To do this successfully the background had to be determined and the outlier intensities had to be extensively filtered prior to the refinement.

The image plate recordings of α-BiB_3O_6 at high pressure were quite spotty (Fig.41(a)) and needed effective filtering before integration to extract the underlying information correctly. A fractile filter removing a fraction of the highest and lowest intensities from each bin was used. The fraction to be removed was determined using the relation of the normal to the normal-Pareto distributed intensities of a strong peak. This resulted in 58% of the highest intensity being removed from each bin before integration (Fig. 41(b)).

This filtering method led to approximately normally distributed intensities, ideally suited for least squares refinement (Figs. 41(c) and(d)). Integration of all data sets was then performed with Powder3D IP, resulting in 19 diagrams of corrected intensities versus the scattering angle 2θ. The crystal structure of ambient α-BiB_3O_6 is highly compressible (bulk modulus of 38(1) GPa) and stable to a pressure of at least $P = 6.09$ GPa. The positional parameters of α-BiB_3O_6 at elevated pressure vary only slightly from the published values at ambient conditions. α-BiB_3O_6 crystallizes in the acentric polar space group $C2$. The crystal structure of α-BiB_3O_6 is built of alternating layers of bismuth atoms and networks of borate groups networks. Two thirds of the borate atoms are trigonally coordinated and one third of the boron atoms are tetrahedrally coordinated, with all four corners of each $[BO4]^{5-}$ tetrahedron connected to a separate $[BO3]^{3-}$ triangle. All $[BO_3]^{3-}$ triangles share two corners with neighboring $[BO_4]^{5-}$ tetrahedra with the remaining oxygen atom bonded exclusively to two bismuth atoms. The trivalent bismuth cations are irregularly coordinated by $4 + 2$ oxygen atoms, formally forming $[BiO_6]$ units sharing six edges with neighboring $[BiO_6]$ units. The effect of the lone pair electrons on the crystal structure is quite visible through open channels down the c^*-axis. The largest convexity of the channels is along the b-axis, which is exactly the direction in which the soft lone-pair electrons of Bi^{+3} point (Fig. 42). The channels are reminiscent of those in the AB_2O_4 type structures in which the lone-pairs of B-atoms cause large channels running through the structure.

The main effect of increasing external pressure on the crystal structure of α-BiB_3O_6 is a strong anisotropic compression of the unit cell (Fig. 43) with the maximum compression along the b-axis due to the soft lone pairs of Bi^{+3} (Fig. 42). Interestingly, the a-axis expands with increasing pressure over the entire range of existence of α-BiB_3O_6. It can be shown that mainly the preferential orientation of the lone electron pair of Bi^{3+} is responsible for this so called 'Nuremberg scissor' effect within the ab-plane.

Between a pressure of $P = 6.09$ GPa and $P = 6.86$ GPa, α-BiB_3O_6 exhibits a first-order phase transition into a considerably stiffer (bulk modulus $B = 114(10)$ GPa) high-pressure phase, called ε-BiB_3O_6 (Fig. 43), whose crystal crystal structure was solved by simulated annealing and energy minimization.

On a first view, the crystal structure of the high-pressure α-phase of BiB_3O_6 is quite similar to that of α-BiB_3O_6. On a closer look, differences can be seen in the small reorientations of the $[BO_3]^{3-}$ triangles and $[BO_4]^{5-}$ tetrahedra, and in the higher coordination of the Bi^{3+} cation.

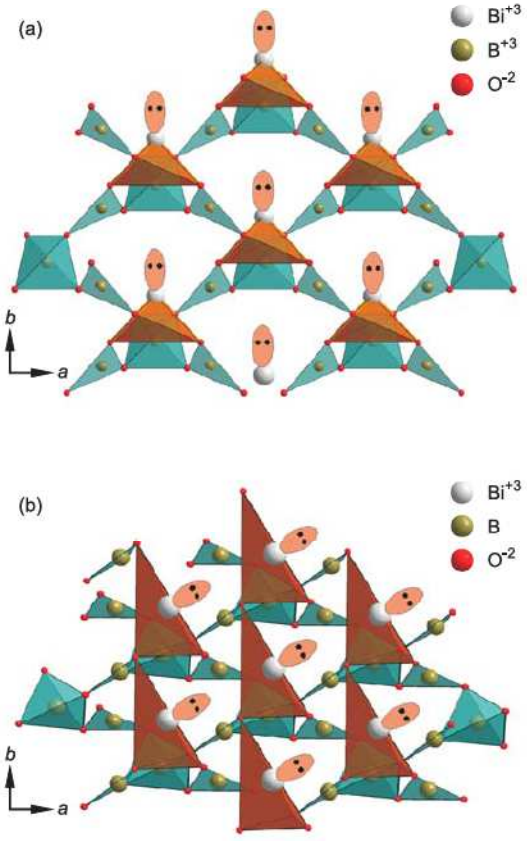

Figure 42: Crystal structures of (a) α-, and (b) ε-bismuth triborate in projections showing the orientation of the free lone pair of Bi^{+3}, symbolized by an ellipse. The BO_4 tetrahedra and BO_3 triangles are drawn in blue, the BO_x polyhedra, showing only real chemical Bi–O bonds, are drawn in red.

The trivalent bismuth cations are now irregularly coordinated by 2 + 6 oxygen atoms, formally forming $[BiO_8]$ polyhedra. The Bi–O separation in two short and four (α-BiB_3O_6) or six (ε-BiB_3O_6) longer bonds suggest the existence of $[|\overline{O}| - \overline{Bi} = O]^{-1}$ groups and thus the presence of the lone pair for the entire pressure range under investigation.

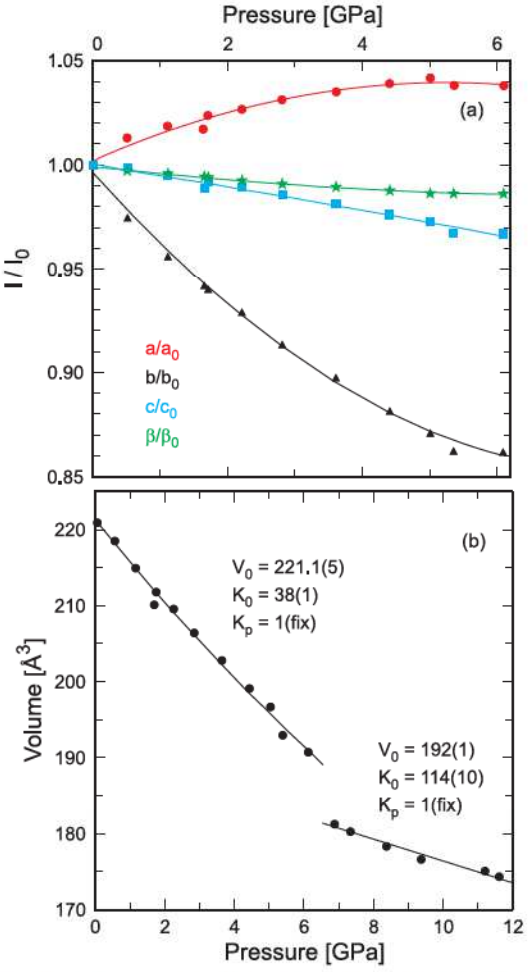

Figure 43: (a): the unit cell volume of α-bismuth triborate (BiB_3O_6) is shown as a function of pressure. The solid lines are those of a Vinet equation of state function fitted to the data points. The bulk modulus (K_0) and volume at ambient pressure (V_0) are given. (b): plot showing the progression of the relative lattice parameters of α-bismuth triborate in dependence on pressure over the stability range of this phase. The lines are guide to the eyes only.

From the observation, that the direction of highest compressibility is along the two-fold axis (*b*-direction) for α-BiB_3O_6, the mechanism of the phase transition at high pressure can be understood. If the pressure is high enough, the space requirement of the electron lone pair can no longer be satisfied. The lone pair can either be forced to adopt spherical *s*-character or evade the pressure by changing its orientation. The latter is responsible for the α- to ε-phase transition of BiB_3O_6 (Fig. 42).

This study shows in particular the supreme importance of high-quality data and data reduction methods to extract Rietveld quality powder diffraction patterns from two-dimensional data with extreme intensity distributions. The accuracy to determine and Rietveld-refine such a crystal structure allowing for the interpretation of minor structural changes was made possible by employing a newly developed sophisticated algorithm for the determination of optimized intensity filters of noisy and spotty 2D powder diffraction images.

Unusual short intermolecular halogen-halogen contacts in chlorinated derivatives of fullerenes

K.Yu. Amsharov, U. Wedig, K.S. Simeonov and M. Jansen

Shortly after the accessibility of C_{60} and C_{70} fullerenes and progress in separation techniques, a number of particular properties of fullerene containing compounds such as superconductivity and ferromagnetism have been discovered. Beside the two members of the fullerene family mentioned above, which are formed almost exclusively during the evaporation of graphite, the fullerene soot contains about 1% of higher fullerenes. However, as it is very difficult to separate individual species in pure form, the chemistry of the higher fullerenes is still poorly explored and the investigation of their properties remained illusive. Moreover, the study of the higher fullerenes is drastically complicated by the existence of several structural isomers. The isomeric diversity, their virtually spherical shape and the rotational mobility cause a very poor quality of fullerene crystals and hamper the structural analysis by X-ray diffraction. Therefor, no ordered crystal structures of pristine fullerenes have been so far reported, except for C_{60} and C_{70}, and most recently, for $C_{84}(14)$ in a cocrystal with silver tetraphenylporphyrin [1].

A feasible way to overcome these problems is the derivatization of the fullerenes. In particular, halogenation has proven to be a versatile and efficient approach for obtaining well crystallized fullerene species. The use of Br_2 in $TiCl_4$ as a highly selective chlorinating agent, allowed us to synthesize a number of high-quality crystals of chlorinated higher fullerenes. Among those are two chiral fullerenes, $C_{76}Cl_{18}$ [2] and $C_{80}Cl_{12}$ [3], and three individual isomers of C_{78}: $C_{78}(2)Cl_{18}$, $C_{78}(3)Cl_{18}$ [4] and $C_{78}(5)Cl_{18}$ [5]. Besides the precise determination of the cage structure of the above mentioned species, detailed analyses of the crystals have clearly demonstrated the presence of numerous short Cl⋯Cl intermolecular contacts (Fig. 44) which are remarkably shorter than the sum of the van-der-Waals radii of two chlorine atoms (3.6 Å).

The formation of short Cl⋯Cl contacts is regarded to be typical for chlorinated aromatic hydrocarbons which are characterized by low C–Cl bond polarity (C–Cl distance of about 1.70–1.73 Å) and rather rare in the case of highly polar C–Cl bonds with C–Cl distances of 1.79–1.81 Å. A proportional relation between C–Cl bond length and bond polarity, however, is not consistent with the observed structures of the chlorinated fullerenes, where the C–Cl bonds are enormously elongated (1.82–1.87 Å). The participation of these Cl atoms in short Cl⋯Cl contacts is highly unexpected, if a significant negative charge is assumed.